Biological Psychiatry

Archival Report

Contribution of the Opioid System to the Antidepressant Effects of Fluoxetine

Elena Carazo-Arias, Phi T. Nguyen, Marley Kass, Hyun Jung Jee, Katherine M. Nautiyal, Valerie Magalong, Lilian Coie, Valentine Andreu, Mark M. Gergues, Huzefa Khalil, Huda Akil, Danusa Mar Arcego, Michael Meaney, Christoph Anacker, Benjamin A. Samuels, John E. Pintar, Irina Morozova, Sergey Kalachikov, and Rene Hen

ABSTRACT

BACKGROUND: Selective serotonin reuptake inhibitors such as fluoxetine have a limited treatment efficacy. The mechanism by which some patients respond to fluoxetine while others do not remains poorly understood, limiting treatment effectiveness. We have found the opioid system to be involved in the responsiveness to fluoxetine treatment in a mouse model for anxiety- and depressive-like behavior.

METHODS: We analyzed gene expression changes in the dentate gyrus of mice chronically treated with corticosterone and fluoxetine. After identifying a subset of genes of interest, we studied their expression patterns in relation to treatment responsiveness. We further characterized their expression through in situ hybridization and the analysis of a single-cell RNA sequencing dataset. Finally, we behaviorally tested mu and delta opioid receptor knockout mice in the novelty suppressed feeding test and the forced swim test after chronic corticosterone and fluoxetine treatment.

RESULTS: Chronic fluoxetine treatment upregulates proenkephalin expression in the dentate gyrus, and this upregulation is associated with treatment responsiveness. The expression of several of the most significantly upregulated genes, including proenkephalin, is localized to an anatomically and transcriptionally specialized subgroup of mature granule cells in the dentate gyrus. We have also found that the delta opioid receptor contributes to some, but not all, of the behavioral effects of fluoxetine.

CONCLUSIONS: These data indicate that the opioid system is involved in the antidepressant effects of fluoxetine, and this effect may be mediated through the upregulation of proenkephalin in a subpopulation of mature granule cells.

https://doi.org/10.1016/j.biopsych.2022.05.030

Anxiety and depressive disorders have a comorbidity of 60%, and together they are the most common mental illnesses in the United States (1). The medications most often prescribed to treat depressive disorders are selective serotonin reuptake inhibitors (SSRIs), such as fluoxetine. Despite being widely used, only one third of patients experience remission after up to 4 months of treatment with SSRIs (2). To understand treatment-resistant depression, more insight is needed into the molecular mechanisms by which SSRIs exert their behavioral effects. While much effort has gone into understanding how the serotonergic system is involved in mediating fluoxetine's effects, insight into the downstream effects and other systems involved will be key in gaining a deeper understanding of fluoxetine's mechanism of action (3).

The opioid system modulates pain processing, endocrine function, and mood regulation, among other functions (4). These functions are mediated through 3 major opioid receptor subtypes—mu opioid receptor (MOR), delta opioid receptor (DOR), and kappa opioid receptor (KOR) —each of them uniquely influencing mood regulation. MOR agonists produce euphoria, and in rodent studies, acute pharmacological activation of the MOR has been shown to reduce depressive-like behaviors (5,6). In contrast, KOR agonists promote depressive-like behaviors, while KOR antagonists induce antidepressant-like effects (7). DOR activation through peptidergic and nonpeptidergic agonists produces anxiolytic and antidepressive-like effects (8–11). Furthermore, mice lacking the DOR gene display higher anxiety-like behavior in the elevated plus maze and the light-dark box test, while mice lacking the MOR gene show a decrease in anxiety levels in those same tasks (12). Opioid receptors are therefore considered a potential target for the mediation of antidepressant effects. In fact, tianeptine, which is an antidepressant commonly used in Europe and South America, has recently been shown to be an agonist of MOR (13), and we have shown that the antidepressant-like effects of tianeptine require the MOR (14). In addition, clinical trials evaluating the efficacy of DOR and MOR agonists or KOR antagonists as antidepressants are currently underway.

Opioid receptors are stimulated by several different endogenous opioid peptides, which bind to opioid receptors with varying affinities. Two types of these endogenous opioid

SEE COMMENTARY ON PAGE 920

 © 2022 Society of Biological Psychiatry.
 ISSN: 0006-3223

peptides, enkephalin and dynorphin, exhibit opposing effects. [Met^5]-enkephalin and [Leu^5]-enkephalin bind preferentially to the DOR and also exhibit a 10-fold lower affinity for the MOR (15). Dynorphin, on the other hand, binds preferentially to the KOR (16). These peptides are generated from the maturation of long precursors, namely prodynorphin (*Pdyn*), which gives rise to [Leu^5]-enkephalin and dynorphin among others, and pro-enkephalin (*Penk*), which gives rise to [Met^5]- and [Leu^5]-enkephalin among others (17). *Penk* has been previously shown to be involved in mood regulation. *Penk*-knockout (KO) mice exhibit exaggerated responses to fearful and anxiety-provoking stimuli (18). Furthermore, administration of an enkephalinase cocktail (which increases endogenous enkephalin levels) can alleviate the effects of chronic social defeat stress (19), while its antidepressive-like effects are blunted in *Penk*-KO mice (20).

While there is accumulating evidence implicating the opioid system in antidepressant mechanisms, it is still poorly understood how this system may be involved in the antidepressant effects of SSRIs. In this study, we analyzed gene expression data from the dentate gyrus (DG) of fluoxetine-treated mice and identified *Penk* and other related genes as important players in the response to fluoxetine. We also show that fluoxetine increases gene expression of *Penk* and other related genes in a subset of mature granule cells (mGC) that are both anatomically and transcriptionally distinct. To further understand the role of *Penk* and the opioid system in the mediation of fluoxetine's effect, we carried out a series of behavioral tasks in MOR-KO and DOR-KO mice treated with fluoxetine and found that the DOR is important in mediating some antidepressant-like effects of fluoxetine.

METHODS AND MATERIALS

Mice

Procedures were conducted in accordance with the U.S. National Institutes of Health Guide for the Care and Use of Laboratory Animals and the New York State Psychiatric Institute Institutional Animal Care and Use Committee at Columbia University and the Research Foundation for Mental Hygiene.

Experimental Mice. MOR-KO and DOR-KO mice were bred in-house. MOR-wild-type (WT) and DOR-WT littermates from heterozygote breedings were used as WT controls. C57BL/6J WT mice were purchased from Taconic Farms. Only male mice were included in the experiments.

Drugs

Corticosterone. Corticosterone (Sigma-Aldrich) (35 μg/mL) was dissolved in vehicle (Veh) (0.45% beta-cyclodextrin; Sigma-Aldrich) and delivered alone or in the presence of antidepressant in opaque bottles to protect it from light. Corticosterone solution was available ad libitum in the drinking water.

Fluoxetine. Fluoxetine hydrochloride (160 μg/mL) was purchased from Anawa Trading and delivered ad libitum in the presence of corticosterone in opaque bottles to protect from light.

Behavioral Testing

Novelty Suppressed Feeding. The novelty suppressed feeding (NSF) test on C57BL/6J WT mice was carried out as previously described (21).

Forced Swim Test. Mice were placed into plastic buckets (19 cm diameter, 23 cm deep, filled with 25 °C water) and run for 5 minutes. Time spent immobile versus swimming and climbing was measured. The forced swim test (FST) and NSF tests were administered on different days.

Gene Expression

The gene expression data of the fluoxetine effects in the DG were obtained using the Affymetrix gene expression analysis platform. The raw data for this study are available at Gene Expression Omnibus accession GSE43261. Sample collection and data preprocessing from this microarray experiment have been previously described by Samuels *et al.* (21).

In Situ Hybridization

Brains from mature male mice were collected and immediately frozen in chilled 2-methylbutane. Brains were sectioned (Leica CM3050 S cryostat) at a thickness of 20 μm, and the slices were thaw mounted on freeze safe slides. In situ hybridization was performed using the RNAscope Fluorescent Multiplex Assay (catalog No. 320851; Advanced Cell Diagnostics, Inc.) and a ready-made probe labeling Penk (catalog No. 318761; Advanced Cell Diagnostics, Inc.). The assay was performed according to the manufacturer's instructions.

For a full description of methods, see Supplemental Methods and Materials in Supplement 1.

RESULTS

Fluoxetine Treatment in the Corticosterone Model for Chronic Stress Elicits a Range of Behaviors

C57BL/6J WT mice were administered corticosterone (5 mg/kg/day) for 4 weeks, which has been shown to result in a behavioral phenotype similar to that elicited by chronic stress (22). Mice were subsequently treated with either fluoxetine (18 mg/kg/day) or Veh for an additional 4 weeks while corticosterone administration continued. These mice were then run in the NSF and FST, behavioral assays that measure anxiety-like and depressive-like phenotypes, respectively. A subset of these mice were selected for ventral DG (vDG) and dorsal DG (dDG) dissection and extraction, and the samples were then run on a microarray Affymetrix gene expression assay (Figure 1A).

Chronic fluoxetine treatment resulted in a significant decrease both in the latency to feed in the NSF test ($p < .0001$) (Figure 1B) and in the time spent immobile in the FST ($p = .0007$) (Figure 1C). Interestingly, there was a significant correlation between the behaviors in the NSF test and FST ($r = 0.5825$, $p = .0004$) (Figure 1D), suggesting that the response levels to fluoxetine of individual mice are consistent across these 2 behavioral paradigms.

These results stand in agreement with previous reports using the chronic corticosterone model for chronic stress followed by fluoxetine treatment (23,24) and support the use of

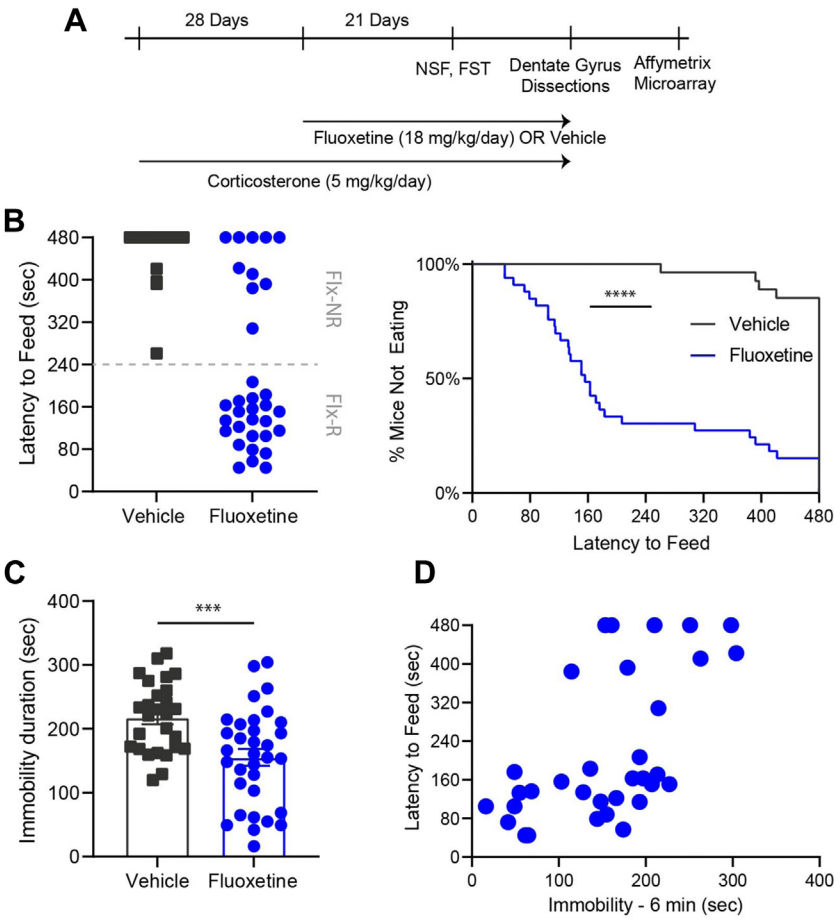


Figure 1. Chronic corticosterone and fluoxetine administration results in treatment response. **(A)** Experimental timeline of treatment administration. **(B)** Total latency to feed per mouse (left) and survival curve (right) of vehicle (gray) and fluoxetine-treated mice (blue). Gray dotted line represents the cutoff point for the definition of treatment responsiveness. Log-rank (Mantel-Cox) test: $\chi^2 = 34.91$, $p < .0001$; $n = 27$ (vehicle), 33 (fluoxetine). **(C)** Total (6 minutes) immobility in FST. Unpaired t test vehicle vs. fluoxetine $p = .0007$. **(D)** Correlation of latency to feed in the NSF and total (6 minutes) immobility in FST of the fluoxetine-treated mice (blue) ($r = 0.5825$, $p = .0004$). Flx-NR, fluoxetine-nonresponders; Flx-R, fluoxetine-responders; FST, forced swim test; NSF, novelty suppressed feeding.

this model as a paradigm that parallels some features of the antidepressant response in humans, in which about 50% of patients fail to respond to treatment with fluoxetine or other SSRIs (2,25).

The response to fluoxetine in both tasks included a wide range of behavioral responses, and when applicable, we have analyzed the behavioral response as a continuous measure. In other cases, we have separated the behavioral response to fluoxetine into treatment responder and nonresponder mice to gain further insight into mechanisms regulating treatment responsiveness. Mice were considered nonresponders when their latency to feed was ≥240 seconds. This cutoff value was defined experimentally by selecting the lowest latency to feed value of the Veh-treated group (Figure 1B).

Chronic Fluoxetine Treatment Increases Proenkephalin Levels in the DG

Previous studies have pointed to the DG as an important region in the mediation of the behavioral response to antidepressants (22,26,27), so we focused our gene expression analysis on this region.

Of all the mice behaviorally tested (Figure 1), only a small subset was selected for further DG tissue samples dissection that were subsequently processed for Afymetrix microarray gene expression analysis. These data have been partially analyzed before (21); here, we report the results of a series of new analyses not previously published.

Differential gene expression analysis was conducted using the GenePattern software ComparativeMarkerSelection tool (28). In both the vDG and dDG, we identified over 200 genes that significantly changed their expression levels (fold change > 1.5, false discovery rate [FDR] < .05) when Veh and fluoxetine-responder (Flx-R) groups were compared (Tables S1–S4 in Supplement 2). *Penk*, an opioid peptide precursor gene, exhibited the highest upregulation in the vDG in Flx-R mice compared with Veh-treated mice (fold change = 12, FDR = .0101) (Figure 2A) and was the fourth highest upregulated gene in the dDG (fold change = 6.4, FDR = .009) (Figure S2A in Supplement 1).

Pdyn, another opioid peptide precursor, was significantly downregulated after fluoxetine treatment in the vDG. Other genes previously found to be relevant for the antidepressant response in the DG were also identified by this analysis, such as *Bdnf*, *Rgs4*, and *Htr4* (Tables S1–S4 in Supplement 2;

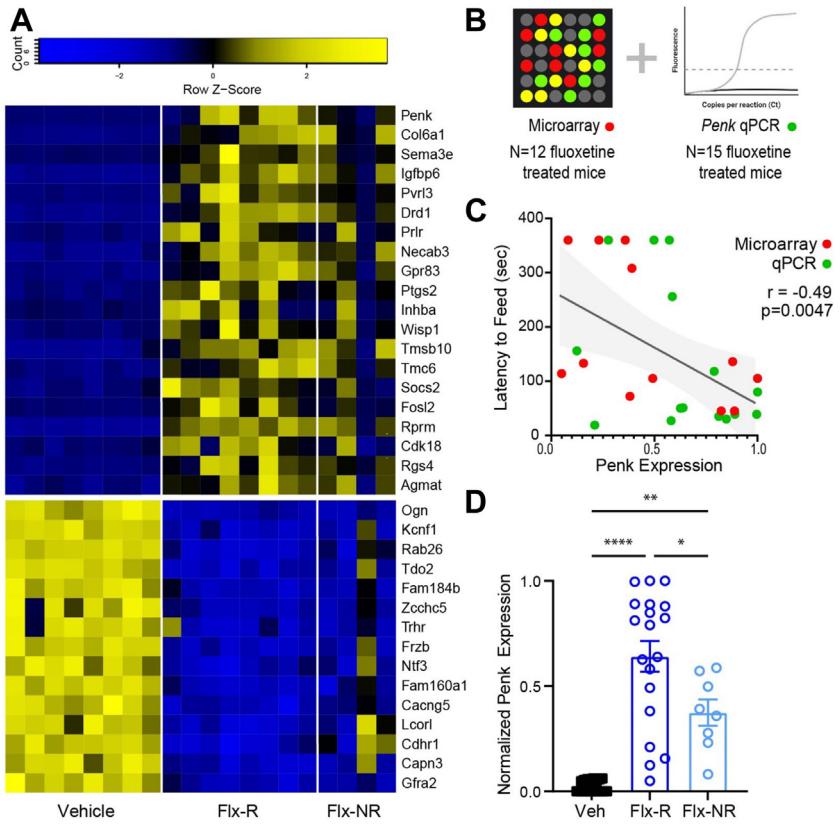


Figure 2. Ventral dentate gyrus microarray results show a significant upregulation of *Penk* in fluoxetine-treated mice. **(A)** Heatmap representing significantly differentially expressed genes (fold change $>$ 2, q value $<$ .05) between vehicle and Flx-R mice in the ventral dentate gyrus. Each row represents the expression of a specific gene (in z score units), and genes are organized from largest (top) to smallest fold change value within each panel. Top panel shows the first 20 most upregulated genes, bottom panel shows the 15 most downregulated genes. **(B)** Cartoon representing the combined microarray and qPCR dataset used for the calculations contained in panels **(C)** and **(D)**. **(C)** *Penk* expression in fluoxetine-treated mice is significantly correlated with the latency to feed in the novelty suppressed feeding test (r = −0.49, p = .0047); n = 27. Each dataset was normalized to maximum *Penk* expression. **(D)** One-way analysis of variance: interaction $F_{2,43}$ = 38.15, p $<$ .0001; Tukey test multiple comparison Veh vs. Flx-R p = .0001, Veh vs. Flx-NR p = .0012, Flx-R vs. Flx-NR p = .0158; n = 19 (Veh), 19 (Flx-R), and 8 (Flx-NR). Flx-NR, fluoxetine-nonresponders; Flx-R, fluoxetine-responders; qPCR, quantitative polymerase chain reaction, Veh, vehicle.

Figures S1A and S2B in Supplement 1). These 3 genes were also found to have gene expression patterns that highly correlated with that of *Penk* (Figures S1B and S2C in Supplement 1).

We then performed an unbiased weighted gene coexpression network analysis (29) to independently identify clusters (modules) of genes with similar patterns of expression. A subset of the identified modules strongly correlated with behavioral outcomes as measured by latency to feed in the NSF and immobility in the FST (Figure 3A). We identified module A as containing *Penk*, *Rgs4*, and *Htr4* (for a full list of genes in module A see Table S5). Within this module, *Penk* displayed the highest module membership and gene significance values (p $<$ .0001 and p = .00012, respectively) (Figure 3B), which measure the correlation of the gene's expression with a trait of interest, in our case, latency to feed in the NSF.

To further study the involvement of *Penk* in the behavioral response to fluoxetine, we treated an additional cohort of mice with chronic corticosterone and fluoxetine (or Veh) and performed a quantitative polymerase chain reaction analysis of *Penk* expression in the DG. *Penk* gene expression values from both the quantitative polymerase chain reaction and the microarray experiments were normalized and combined (Figure 2A). Using this combined dataset, we found *Penk* expression to be significantly correlated with the latency to feed in the NSF test in fluoxetine-treated mice (p = .0047) (Figure 2B, C). *Penk* expression was also significantly different between Flx-R and Flx-nonresponder mice (p = .0358) (Figure 2D).

To validate our results using a different paradigm, we collected an independent RNA sequencing (RNA-seq) dataset studying the effects of fluoxetine in mice with a mixed genetic background. In this study, mice were not treated with corticosterone, but instead were chronically stressed through the administration of chronic oral gavage (water vs. fluoxetine gavage). In this dataset, we were able to corroborate the upregulation of key genes of interest after fluoxetine treatment in this sample such as *Penk*, *Rgs4*, *Col6a1*, and *Necab3* in the vDG. Unfortunately, in this low stress paradigm, most animals responded to fluoxetine, thereby not allowing us to compare responders and nonresponders (Figure S3 in Supplement 1).

Combined, these data strongly indicate that the expression pattern of *Penk* is strongly correlated with the behavioral response to fluoxetine and suggest, therefore, that upregulation of *Penk* contributes to treatment responsiveness.

Fluoxetine Upregulates Genes in a Distinct Subpopulation of mGC in the DG

We performed RNAscope in situ hybridization on mice treated with Veh or fluoxetine to quantify how *Penk* messenger RNA expression varies across brain regions (Figure 4A). *Penk* was significantly upregulated after chronic fluoxetine treatment in

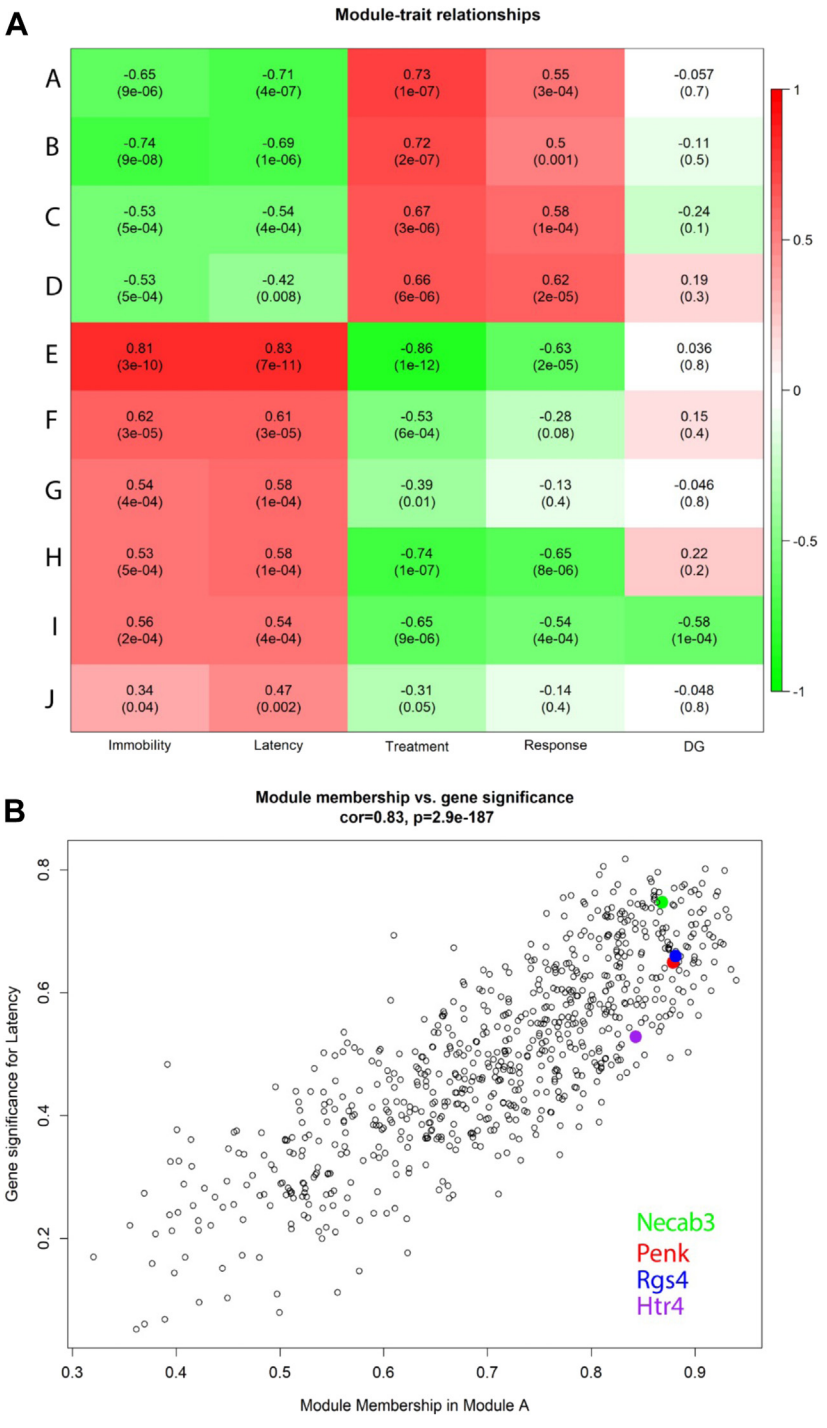


Figure 3. Weighted gene coexpression network analysis of gene expression data identifies *Penk*-containing module as significantly correlated with latency to feed in the novelty suppressed feeding. **(A)** Correlation of a subset of identified modules through weighted gene coexpression network analysis. Top values in each square represents correlation value between a given module (y-axis) and a trait (x-axis); bottom value represents the significance of this correlation. Traits displayed on the x-axis: immobility in the forced swim test, latency to feed in the novelty suppressed feeding, treatment (fluoxetine or vehicle), response (fluoxetine-responders, fluoxetine-nonresponders, or no treatment), DG (dorsal or ventral). Each square is colored based on the correlation value as depicted on the right-hand scale: red indicates a direct correlation, green indicates an inverse correlation. For example, in module A, higher latency to feed is correlated with lower expression. **(B)** Scatter plot of genes belonging to module A as a function of the gene significance for latency to feed and the module membership values for each gene within the module. Highlighted genes: green: *Necab3*, red: *Penk*, blue: *Rgs4*, purple: *Htr4*. DG, dentate gyrus.

the DG (Figure 4B) (p = .00016 and p = .00009, respectively), as well as, to a smaller extent, in the entorhinal cortex (p = .00343), but not in the piriform cortex, basolateral amygdala, lateral hypothalamus, CA1, or CA3 (Figure 4D). The expression level of *Penk* within the DG was strongest in the upper blade and mostly limited to the uppermost layer of the granule cell layer, closest to the inner molecular layer, as well as in some cells within the inner molecular layer itself (Figure 4C).

To further map *Penk* and other genes of interest to specific cellular subpopulations within the DG, we reanalyzed a

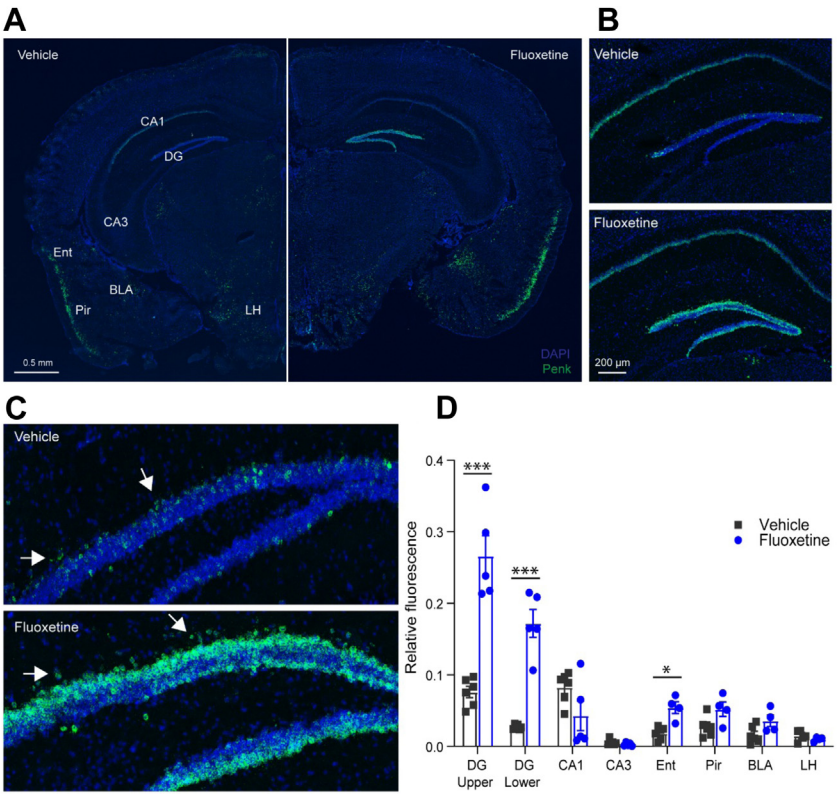


Figure 4. *Penk* messenger RNA expression quantification across brain regions. **(A)** Representative 10× slices of *Penk* expression measured through RNAscope of a vehicle and a fluoxetine-treated mouse. Green staining shows *Penk*; blue staining is DAPI. **(B)** Representative 20× fluorescent images of the dorsal DG of vehicle and fluoxetine-treated mice. **(C)** Close up representative image of Penk pattern of expression in the DG. White arrows represent cell bodies of mature granule cells in the inner molecular layer. **(D)** Quantification of Penk expression across the brain regions marked in Figure 4A. Unpaired *t* test after false discovery rate correction (Benjamini, Krieger, Yekutieli): upper DG $p = .000158$; lower DG $p = .00009$; Ent $p = .003427$. BLA, basolateral amygdala; DG, dentate gyrus; Ent, entorhinal cortex; LH, lateral hypothalamus; Pir, piriform cortex.

previously published single-cell RNA-seq dataset (30) and identified 7 main cell clusters corresponding to distinct cell types within the DG, which is overall consistent with published results (30,31). Three of these clusters belonged to mGC, such as the mGC3 cluster (Figure 5A). Differential expression analysis performed on the 25 cells belonging to the mGC3 cluster identified 53 significant gene markers unique to this population of mGCs (area under the receiver operator curve > 0.72 and FDR $< .05$) (Figure 5; Figures S5 and S6 in Supplement 1). Some of the most significantly upregulated gene markers for the mGC3 cluster included *Penk*, *Rgs4*, *Necab3*, and *Col6a1* (Figure 5B–E; Figure S5 in Supplement 1). However, not all of the differentially expressed genes identified by the microarray analysis showed such specific clustering. For example, *Bdnf* expression was more uniformly distributed throughout all granule cell clusters (Figure 5F).

Finally, we performed an enrichment analysis to study how the expression patterns of the genes found in module A might correspond to the cell types identified. This enrichment analysis showed that the top 100 genes of module A map onto the same cells that contain mGC3 cluster cell markers. Therefore, expression patterns of the top *Penk* coexpressed genes contain an expression signature that is characteristic of the mGC3 cluster (Figure 5G).

Our findings related to the spatial localization of *Penk* transcription within the DG are in good agreement with a recent report (31) and point to the existence of a specialized subpopulation of mGCs expressing many other genes we found to be upregulated by fluoxetine. Together with the anatomically distinct clustering of granule cells expressing *Penk* (Figure 4C), our data suggest that fluoxetine upregulates a specific transcriptional program (most prominently *Penk*, *RGS4*, *Necab3*, and *Col6a1*) in an anatomically and transcriptionally distinct subpopulation of mGC.

The DOR Contributes to the Behavioral Effects of Fluoxetine in the FST

The *Penk* gene transcript gives rise to enkephalin peptides that bind preferentially to the DOR and, to a lesser extent, to the MOR. Because we showed that chronic fluoxetine treatment increases *Penk* expression in the DG, we investigated whether the DOR and MOR play a role in the mediation of fluoxetine's antidepressant effects. MOR-KO and DOR-KO mice were treated chronically with corticosterone, followed by fluoxetine (or Veh) and then subjected to a battery of behavioral tasks measuring anxiety- and depression-like phenotypes (Figure 6A). Both MOR-KO and WT control littermates displayed a decreased immobility in the FST after chronic fluoxetine treatment (two-way analysis of variance [ANOVA] with significant effect of treatment factor [$p = .0132$] but not genotype factor [$p = .2847$] or interaction [$p = .9711$]) (Figure 6B). In contrast, DOR-KO mice had an attenuated response to fluoxetine in the FST compared with their WT control littermates (two-way ANOVA with significant effect of treatment factor [$p = .0003$] and genotype factor [$p = .0133$], but no

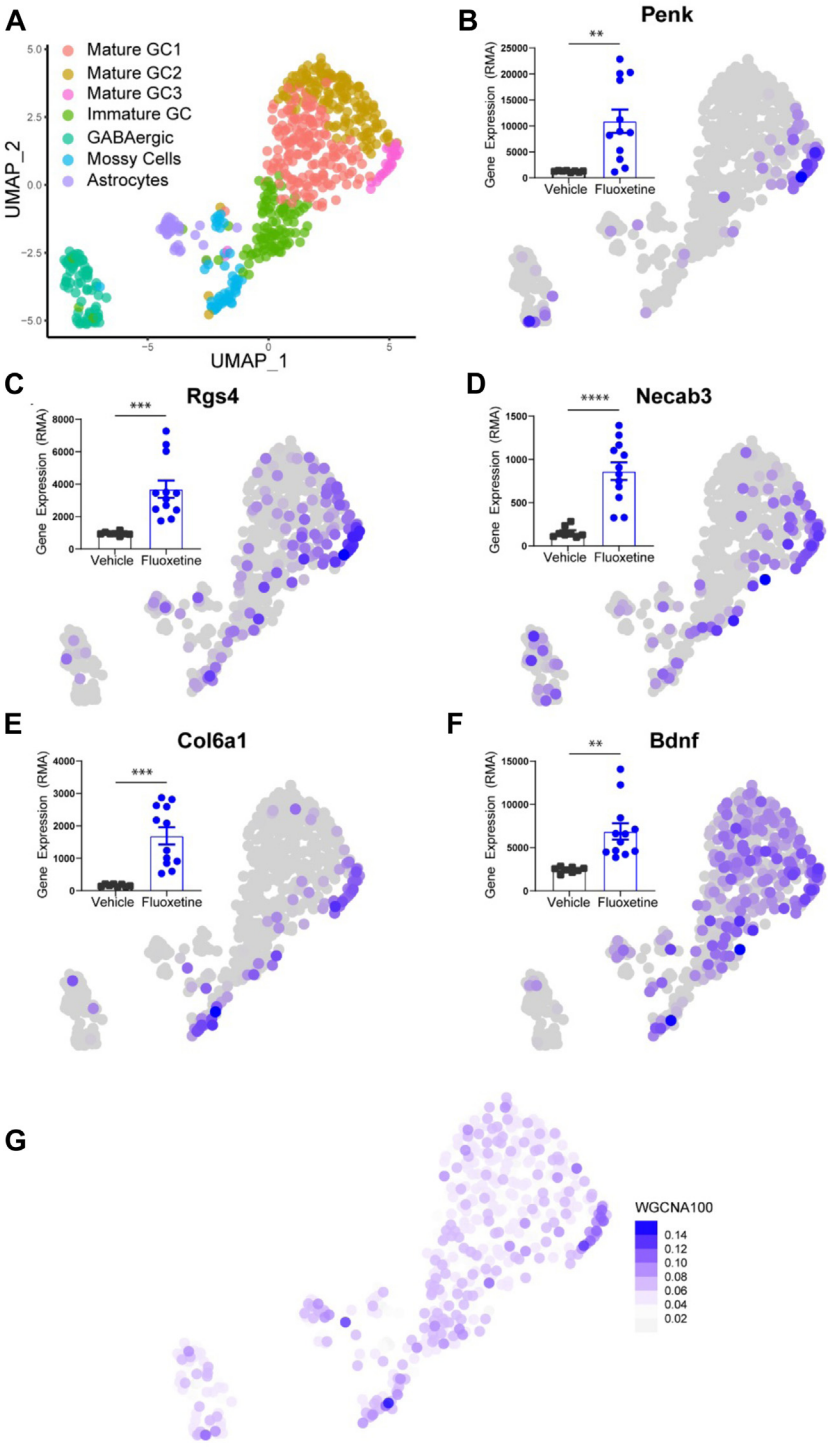


Figure 5. Subset of fluoxetine upregulated genes localized in a discreet population of mature GCs. **(A)** Identification of cell population clusters using the dimensionality reduction algorithm UMAP on a previously published single-cell RNA sequencing dentate gyrus dataset (30). Each circle represents a single cell. Cell type assignments for each identified cluster are shown in different colors. **(B–F)** Expression of fluoxetine upregulated genes within the different cell clusters identified. Higher expression of a given gene in a specific single cell is represented by a darker purple. The inset on the top left corner of each panel represents RMA-normalized gene expression values for individual genes that were identified in our microarray analysis. Unpaired *t* test: *Penk* $p = .0026$; *Rgs4* $p = .0006$; *Necab3* $p < .0001$; *Col6a1* $p = .0002$; *Bdnf* $p = .0013$; $n = 8$ (vehicle), 12 (fluoxetine). **(G)** Data represents the AUCell scores of the top 100 most significant genes found in the identified WGCNA module A. Genes are plotted (mapped) onto the dentate gyrus small nuclear RNA sequencing data. GABAergic, gamma-aminobutyric acidergic; GC, granule cell; RMA, robust multiarray average; UMAP, uniform manifold approximation and projection; WGCNA, weighted gene coexpression network analysis.

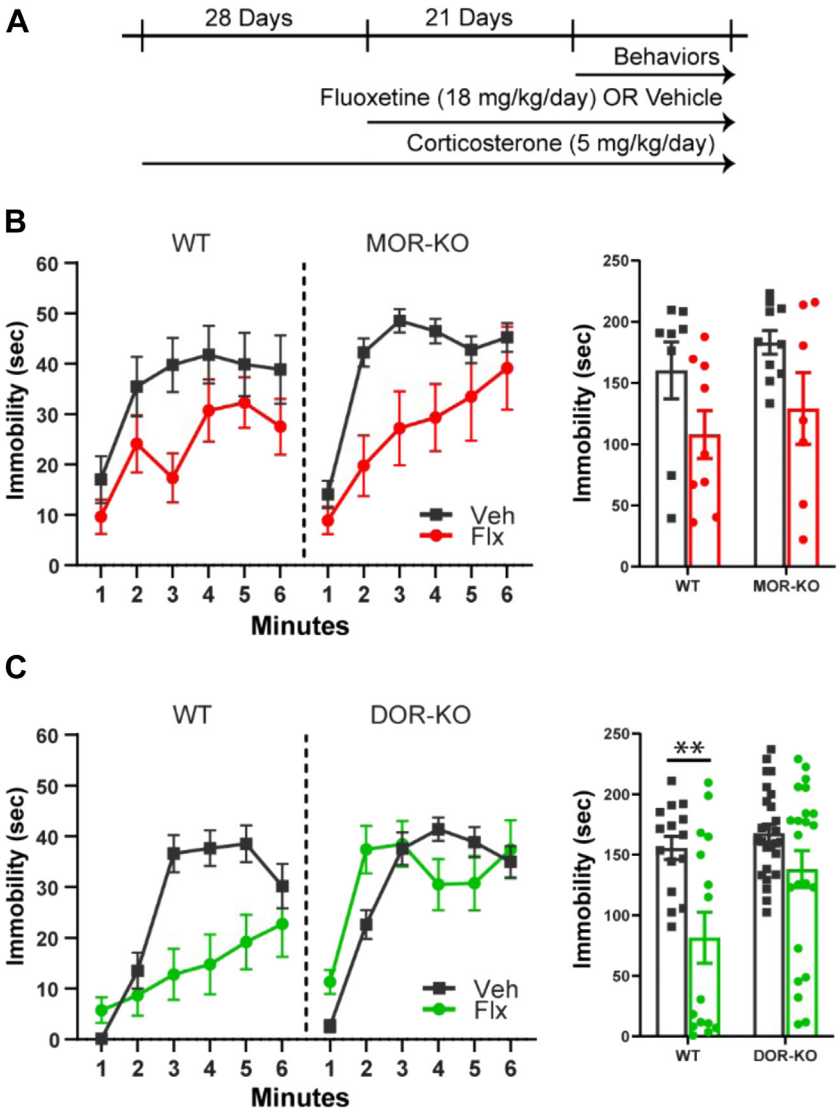


Figure 6. Behavioral effect of fluoxetine in the FST in MOR-KO but not DOR-KO mice. **(A)** Timeline of corticosterone and fluoxetine treatment for MOR-KO and DOR-KO mice. **(B)** Antidepressant-like effect of fluoxetine in MOR-KO mice in the FST. Two-way analysis of variance: interaction $F_{1,30} = 0.001$, $p = .9711$; genotype $F_{1,30} = 1.187$, $p = .2847$; treatment $F_{1,30} = 6.937$, $p = .013$; $n = 8$ (Veh), 9 (WT-Flx), 10 (MOR KO-Veh), and 7 (MOR KO-Flx). Left: average immobility time per minute, right: total immobility during the last 4 minutes of the FST. **(C)** No antidepressant-like effect of fluoxetine in DOR-KO mice in the FST. Two-way analysis of variance: interaction $F_{1,74} = 2.675$, $p = .1062$; genotype $F_{1,74} = 6.433$, $p = .013$; treatment $F_{1,74} = 14.71$, $p = .0003$; planned comparison t test, WT vehicle vs. fluoxetine, $p = .0016$; $n = 15$ (WT-Veh), 15 (WT-Flx), 26 (DOR KO-Veh), and 22 (DOR KO-Flx). Left: average immobility time per minute, right: total immobility during the last 4 minutes of the FST. DOR, delta opioid receptor; Flx, fluoxetine; FST, forced swim test; KO, knockout; MOR, mu opioid receptor; Veh, vehicle; WT, wild-type.

interaction [$p = .1062$]) (Figure 6C). However, in the NSF test, both MOR-KO and DOR-KO mice responded in the same way as WT (Figure S4 in Supplement 1). These results, taken together, point to the contribution of DOR to some but not all of the behavioral effects of fluoxetine.

Fluoxetine Treatment Increases Neurogenesis in Both WT and DOR-KO Mice

We have shown previously that chronic SSRI treatment increases neurogenesis in the DG, and that neurogenesis mediates some of the behavioral effects of fluoxetine (26). We also have shown that ablating neurogenesis blocks the behavioral effect of fluoxetine in the NSF test, but not in the FST (22). Therefore, we assessed neurogenesis levels in the DG of fluoxetine-treated WT and DOR-KO mice.

We performed an immunohistochemical analysis of the immature neuron marker doublecortin in DOR-KO and WT control littermates that had been treated with chronic corticosterone and fluoxetine (or Veh) (Figure 7A). In the vDG, fluoxetine increased neurogenesis in both the DOR-KO and WT control littermates (two-way ANOVA with significant effect of treatment factor [$p = .01$] but not genotype factor [$p = .7292$] or interaction [$p = .7095$]) (Figure 7B). The same effect of treatment (but not genotype) on the neurogenesis level was observed in the dDG (two-way ANOVA with significant effect of treatment factor [$p = .03$] but not genotype factor [$p = .5919$] or interaction [$p = .7086$]) (Figure 7C).

This result suggests that the contribution of the DOR to the behavioral effects of fluoxetine in the FST is not mediated by neurogenesis, corroborating previous evidence showing that the FST, as opposed to the NSF, is a neurogenesis-independent behavior (22).

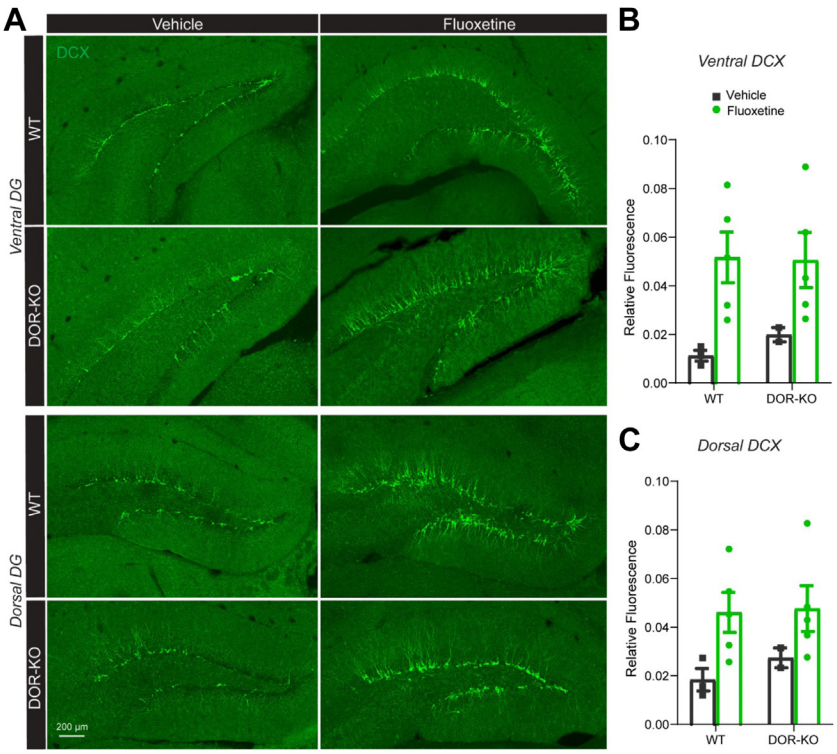


Figure 7. Fluoxetine treatment increases neurogenesis in both WT and DOR-KO mice. **(A)** Confocal 20× images of vDG (top 4) and dDG (bottom 4) *DCX* antibody staining in the DG. **(B, C)** *DCX* (green) fluorescence represented as a normalized pixel count value. **(B)** vDG two-way analysis of variance: interaction $F_{1,11}$ = 0.1462, p = .7095; genotype $F_{1,11}$ = 0.1261, p = .7292; treatment $F_{1,11}$ = 9.419, p = .0107. **(C)** dDG two-way analysis of variance: interaction $F_{1,11}$ = 0.1471, p = .7086; genotype $F_{1,11}$ = 0.3048, p = .5919; treatment $F_{1,11}$ = 6.262, p = .0294; n = 3 (WT-vehicle), 5 (WT-Flx), 2 (DOR KO-vehicle), and 5 (DOR KO-Flx). DG, dentate gyrus; DOR, delta opioid receptor; Flx, fluoxetine; KO, knockout; WT, wild-type.

DISCUSSION

Despite their widespread use, treatments with SSRIs still present many challenges, such as undesirable side effects, delayed onset of effect, and treatment nonresponsiveness. In fact, up to two thirds of patients do not experience remission of symptoms after first-line treatment with SSRIs (2). In this study, we aimed to better understand what molecular mechanisms underpin treatment efficacy.

We showed here that the corticosterone model for chronic stress followed by fluoxetine treatment in C57BL/6J mice appears to be a useful tool to induce a range of antidepressant responses, much like those found in human patients.

Analysis of the DG microarray gene expression data revealed that *Penk* is significantly upregulated in both the vDG and dDG in Flx-R mice compared with Veh-treated mice, as well as a significant difference in expression between Flx-R and fluoxetine nonresponders. In fact, upregulation of *Penk* in the DG after chronic SSRI treatment has been previously reported (32) and our group also confirmed this finding through RNA-seq in an independent experiment (Figure S3 in Supplement 1). Furthermore, a similar upregulation of *Penk* was observed after environmental enrichment, which is another paradigm shown to elicit anxiolytic- and antidepressant-like effects (33).

In situ hybridization using RNAscope revealed that *Penk* expression after fluoxetine treatment is indeed highest in the DG as compared with other brain regions and appears to be restricted to a subpopulation of granule cells located preferentially within the upper blade of the DG, close to the border between the granule cell layer and the inner molecular layer (Figure 4B). This pattern of expression is highly reminiscent of the localization of semilunar granule cells (SGCs), a subpopulation of mGC with distinct morphological, anatomical, and electrophysiological properties that has been identified in the past years (31,34,35). Furthermore, a recent study finding *Penk* to be a marker for highly active granule cells in the DG also highlighted the parallels between *Penk*$^+$ neurons and SGCs (31), pointing to a potential overlap between these 2 populations of neurons.

This population of *Penk*$^+$ neurons is not only anatomically distinct, but transcriptionally differentiated as well. Our analysis of a previously published single-cell RNA-seq dataset (30) reveals that *Penk*$^+$ neurons belong to a distinct transcriptional cluster of mGC, which we termed mature GC3 (mGC3). This mGC3 cluster not only preferentially expresses *Penk*, but also a number of other unique marker genes that we have found to be upregulated by fluoxetine, such as *Necab3*, *Col6a1*, and *Rgs4* (Figures 2A and 5; Figure S5 in Supplement 1). Furthermore, *Penk*, *Necab3*, *Rgs4*, and *Htr4* were all also identified within module A of the weighted gene coexpression network analysis (Figure 3B). Interestingly, several of these genes were recently associated with the same distinct population of granule cells and were associated with behaviorally recruited GC activation (31), pointing to a potentially new understanding of the complexity of GC function. In addition, BDNF, which is an established mediator of the antidepressant response in the DG, while being widely expressed throughout all mGC clusters in the DG also has the highest expression in the mGC3 (Figure 5F; Table S6 in Supplement 2).

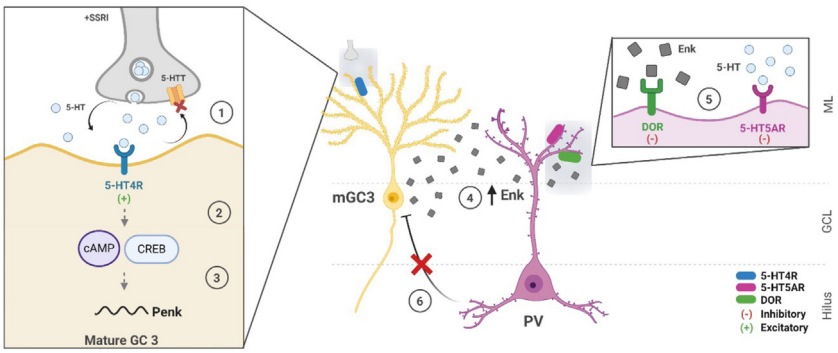


Figure 8. Proposed mechanism of opioid system involvement in the DG circuitry after SSRI treatment. 1) SSRIs block reuptake of serotonin by the serotonin transporter and thus increase synaptic availability of serotonin. 2) Increased serotonin binds to postsynaptic serotonin receptors (5-HT4R in mGC3 and 5-HT5AR in PV interneurons). Receptors coupled to inhibitory G-proteins are labeled with red minus sign, while receptors coupled to excitatory G-proteins are labeled with a green plus sign. 3) Following 5-HT4R activation, cAMP/CREB signaling may be increased, which may lead to increased *Penk* expression and an increased release of Enk, which binds to DOR on PV interneurons. 4) Activation of DOR by Enk and 5-HT5AR by serotonin may lead to an inhibitory effect in PV interneurons, which in turn may result in disinhibition of mGC3 cells. 5-HT4R, 5-HT_4 receptor; 5-HT5AR, 5-HT_{5A} receptor; cAMP/CREB, cyclic adenosine monophosphate/cAMP response element binding protein; DG, dentate gyrus; DOR-KO, delta opioid receptor knockout; Enk, enkephalin; GCL, granule cell layer; mGC, mature granule cell; ML, molecular layer; PV, parvalbumin; SSRI, selective serotonin reuptake inhibitor.

We therefore hypothesize that the antidepressant effect of chronic fluoxetine is mediated by upregulation of *Penk* expression in this highly specialized group of *Penk*$^+$ mGCs that are anatomically and transcriptionally distinct and are preferentially recruited by a variety of behavioral paradigms (31,36). Our results stand in contrast to the long-held view that mGCs in the DG are homogeneous in their properties and anatomy (37) and point to the need for a better understanding of mGC complexity.

Recent evidence has shown that existing antidepressants can act through the opioid system. For example, tianeptine acts through the MOR (14), and recent work has shown that ketamine recruits the opioid system downstream of the activation of glutamate receptors (38–40). The possibility of the DOR being a mediator of antidepressant effects has also been studied extensively in animal models (8–11), and some DOR agonists have even been tested in clinical trials as potential novel antidepressants, although with limited success (41).

In this study, we showed that the DOR may be mediating the behavioral effects of fluoxetine in the FST but not in the NSF test and that the DOR does not appear to mediate the effects of fluoxetine on neurogenesis (42). While both the NSF test and the FST are behavioral tasks with established predictive validity in the study of antidepressant efficacy (43,44), we have previously shown that the behavioral effects of fluoxetine require adult hippocampal neurogenesis in the NSF test, but not in the FST (22). These studies therefore suggest that the behavioral effects of fluoxetine in the NSF test and FST are mediated by distinct mechanisms (45,46).

We propose the following model to explain the contribution of enkephalins in the DG to the effects of a chronic fluoxetine treatment (Figure 8). After the inhibition of serotonin reuptake caused by fluoxetine, several postsynaptic serotonin receptors are involved in mediating the immediate effects of this increase in serotonin availability. Our data show that *Htr5a* and *Htr4* are upregulated, while *Htr1A* is downregulated in the vDG after chronic fluoxetine treatment (Figure S1A in Suppplement 2). Both *Htr1A* and *Htr4* are expressed in mGCs in the DG and have also been shown to contribute to the effects of fluoxetine (27,47). The upregulation of the excitatory *Htr4* in the mGC3 cells upon chronic fluoxetine administration likely results in an increase in cAMP/CREB (cyclic adenosine monophosphate response element binding protein) signaling, which will, in turn, result in increased expression of *Penk* (48). Upregulation of *Penk* in mGC3 cluster may lead to an increased secretion of enkephalins from these granule cells, which will in turn bind to postsynaptic DOR located primarily in GABAergic (gamma-aminobutyric acidergic) parvalbumin interneurons (49). Parvalbumin interneurons in the DG also express the inhibitory receptor *Htr5a*, which we also found to be significantly upregulated after fluoxetine treatment (Figure S1A in Supplement 1). *Htr5a* has been shown to contribute to the antidepressant effects of fluoxetine in the hippocampus through the hyperpolarization of parvalbumin interneurons (50). Altogether we may therefore expect an increase in the activity of mGC3 cells in response to chronic fluoxetine.

SGCs have been shown to generate long-duration plateau potentials in response to excitatory synaptic input, which in turn leads to persistent firing in hilar mossy cells. This increased hilar firing then triggers functional inhibition of regular mGCs (51). Therefore, if mGC3 cells indeed overlap in their identity with SGCs, the activation of this population of GCs after fluoxetine treatment may lead to an inhibition of the larger mGC population, in accordance with recently published studies (24).

Future studies will be aimed at studying the function of mGC3 cells and whether they can be targeted to produce antidepressant effects in patients who do not respond to SSRIs.

ACKNOWLEDGMENTS AND DISCLOSURES

This work was supported by National Institutes of Health (Grant Nos. R37 MH068542, R01 MH083862, R01 AG043688, R01 NS081203, and T32 MH01574 [to RH]). EC-A and RH were supported by New York State Stem Cell Science (Grant No. C029157) and by the Hope for Depression Research Foundation (Grant No. RGA-13-003). SK, IM, and RH were supported by the Seed Grant from Columbia University Data Science Institute. JP and RH were also supported by the National Institutes of Health (Grant No. R21 MH116462). HA and HK were supported by Hope for Depression Research Foundation, NABARD Infrastructure Development Assistance (Grant Nos. U01DA043098 and ONR 00014-19-1-2149). MM and DA were supported by Hope for Depression Research Foundation.

EC-A, PTN, and RH wrote the manuscript. EC-A, PTN, KMN, MK, and RH designed experiments. BAS performed Affymetrix microarray and differential expression analysis. VM performed MOR-KO behavioral

experiment. EC-A, MK, HJ, and VA performed DOR-KO behavioral experiment. EC-A, MK, and LC performed in situ hybridization. EC-A performed immunohistochemistry, cell quantification and weighted gene coexpression network analysis. IM and SK performed correlation analysis and single-cell RNA-seq analysis. HJ performed manual scoring of forced swim test data and cell quantification. PTN, HA, and HK contributed to the analysis of gene expression data. MM and DMA studied the expression of *Penk*-related genes in mouse and human samples. JP provided MOR- and DOR-KO mice.

All data are available in the manuscript or the supplementary materials.

The authors report no biomedical financial interests or potential conflicts of interest.

ARTICLE INFORMATION

From the Department of Biological Sciences (EC-A); Department of Psychiatry (PTN, MK, CA, RH); Department of Neuroscience (LC, VA, RH); Center for Genome Technology and Biomolecular Engineering (IM, SK); Department of Chemical Engineering (IM, SK); Data Science Institute (SK); and Department of Pharmacology (RH), Columbia University; Division of Integrative Neuroscience (EC-A, PTN, MK, HJJ, RH), New York State Psychiatric Institute, New York, New York; Department of Psychological and Brain Sciences (KMN), Dartmouth College, Hanover, New Hampshire; Program in Developmental Neurogenetics (VM), The Saban Research Institute, Children's Hospital Los Angeles, Los Angeles, California; Department of Psychology (MMG, BAS); Department of Neuroscience & Cell Biology (JEP), Rutgers University, New Brunswick, New Jersey; Molecular and Behavioral Neuroscience Institute (HK, HA); Department of Psychiatry (HK, KA), University of Michigan, Ann Arbor, Michigan; Department of Psychiatry (DMA, MM), Faculty of Medicine; Sackler Program for Epigenetics and Psychobiology (MM), Douglas Hospital Research Centre, McGill University, Montreal, Québec, Canada; and Singapore Institute for Clinical Sciences (MM), Singapore.

Address correspondence to Rene Hen, Ph.D., at rh95@cumc.columbia.edu.

Received Dec 16, 2020; revised May 17, 2022; accepted May 18, 2022.

Supplementary material cited in this article is available online at https://doi.org/10.1016/j.biopsych.2022.05.030

REFERENCES

1. Kessler RC, Petukhova M, Sampson NA, Zaslavsky AM, Wittchen H-U (2012): Twelve-month and lifetime prevalence and lifetime morbid risk of anxiety and mood disorders in the United States. Int J Methods Psychiatr Res 21:169–184.
2. Trivedi MH, Rush AJ, Wisniewski SR, Nierenberg AA, Warden D, Ritz L, *et al.* (2006): Evaluation of outcomes with citalopram for depression using measurement-based care in STAR*D: Implications for clinical practice. Am J Psychiatry 163:28–40.
3. Akil H, Gordon J, Hen R, Javitch J, Mayberg H, McEwen B, *et al.* (2018): Treatment resistant depression: A multi-scale, systems biology approach. Neurosci Biobehav Rev 84:272–288.
4. Browne CA, Lucki I (2019): Targeting opioid dysregulation in depression for the development of novel therapeutics. Pharmacol Ther 201:51–76.
5. Besson A, Privat AM, Eschalier A, Fialip J (1996): Effects of morphine, naloxone and their interaction in the learned-helplessness paradigm in rats. Psychopharmacology 123:71–78.
6. Berrocoso E, Ikeda K, Sora I, Uhl GR, Sánchez-Blázquez P, Mico JA (2013): Active behaviours produced by antidepressants and opioids in the mouse tail suspension test. Int J Neuropsychopharmacol 16:151–162.
7. Mague SD, Pliakas AM, Todtenkopf MS, Tomasiewicz HC, Zhang Y, Stevens WC Jr, *et al.* (2003): Antidepressant-like effects of kappa-opioid receptor antagonists in the forced swim test in rats. J Pharmacol Exp Ther 305:323–330.
8. Vergura R, Balboni G, Spagnolo B, Gavioli E, Lambert DG, McDonald J, *et al.* (2008): Anxiolytic- and antidepressant-like activities of H-Dmt-Tic-NH-CH(CH2-COOH)-Bid (UFP-512), a novel selective delta opioid receptor agonist. Peptides 29:93–103.
9. Saitoh A, Kimura Y, Suzuki T, Kawai K, Nagase H, Kamei J (2004): Potential anxiolytic and antidepressant-like activities of SNC80, a selective delta-opioid agonist, in behavioral models in rodents. J Pharmacol Sci 95:374–380.
10. Torregrossa MM, Jutkiewicz EM, Mosberg HI, Balboni G, Watson SJ, Woods JH (2006): Peptidic delta opioid receptor agonists produce antidepressant-like effects in the forced swim test and regulate BDNF mRNA expression in rats. Brain Res 1069:172–181.
11. Naidu PS, Lichtman AH, Archer CC, May EL, Harris LS, Aceto MD (2007): NIH 11082 produces anti-depressant-like activity in the mouse tail-suspension test through a delta-opioid receptor mechanism of action. Eur J Pharmacol 566:132–136.
12. Melo I, Drews E, Zimmer A, Bilkei-Gorzo A (2014): Enkephalin knockout male mice are resistant to chronic mild stress. Genes Brain Behav 13:550–558.
13. Gassaway MM, Rives ML, Kruegel AC, Javitch JA, Sames D (2014): The atypical antidepressant and neurorestorative agent tianeptine is a μ-opioid receptor agonist. Transl Psychiatry 4:e411.
14. Samuels BA, Nautiyal KM, Kruegel AC, Levinstein MR, Magalong VM, Gassaway MM, *et al.* (2017): The behavioral effects of the antidepressant tianeptine require the mu-opioid receptor. Neuropsychopharmacology 42:2052–2063.
15. Mansour A, Hoversten MT, Taylor LP, Watson SJ, Akil H (1995): The cloned mu, delta and kappa receptors and their endogenous ligands: Evidence for two opioid peptide recognition cores. Brain Res 700:89–98.
16. Benarroch EE (2012): Endogenous opioid systems: Current concepts and clinical correlations. Neurology 79:807–814.
17. Johnston ST, Parylak SL, Kim S, Mac N, Lim CK, Gallina IS, *et al.* (2021): AAV ablates neurogenesis in the adult murine hippocampus. eLife 10:e59291.
18. Gibson A, Hart SL, Shabib A (1980): Leucine-enkephalin and methionine-enkephalin produce opposing effects on plasma corticosterone levels in ether-stressed mice. Br J Pharmacol 70:509–511.
19. Nam H, Chandra R, Francis TC, Dias C, Cheer JF, Lobo MK (2019): Reduced nucleus accumbens enkephalins underlie vulnerability to social defeat stress. Neuropsychopharmacology 44:1876–1885.
20. Noble F, Benturquia N, Bilkei-Gorzo A, Zimmer A, Roques BP (2008): Use of preproenkephalin knockout mice and selective inhibitors of enkephalinases to investigate the role of enkephalins in various behaviours. Psychopharmacol (Berl) 196:327–335.
21. Samuels BA, Leonardo ED, Dranovsky A, Williams A, Wong E, Nesbitt AM, *et al.* (2014): Global state measures of the dentate gyrus gene expression system predict antidepressant-sensitive behaviors. PLoS One 9:e85136.
22. David DJ, Samuels BA, Rainer Q, Wang JW, Marsteller D, Mendez I, *et al.* (2009): Neurogenesis-dependent and -independent effects of fluoxetine in an animal model of anxiety/depression. Neuron 62:479–493.
23. Dieterich A, Srivastava P, Sharif A, Stech K, Floeder J, Yohn SE, Samuels BA (2019): Chronic corticosterone administration induces negative valence and impairs positive valence behaviors in mice. Transl Psychiatry 9:337.
24. Yohn CN, Dieterich A, Maita I, Bazer AS, Diethorn E, Ma D, *et al.* (2020): Behavioral response to fluoxetine in both female and male mice is modulated by dentate gyrus granule cell activity. Neurobiol Stress 13:100257.
25. Samuels BA, Leonardo ED, Gadient R, Williams A, Zhou J, David DJ, *et al.* (2011): Modeling treatment-resistant depression. Neuropharmacology 61:408–413.
26. Breitfeld J, Scholl C, Steffens M, Laje G, Stingl JC (2017): Gene expression and proliferation biomarkers for antidepressant treatment resistance. Transl Psychiatry 7:e1061.
27. Samuels BA, Anacker C, Hu A, Levinstein MR, Pickenhagen A, Tsetsenis T, *et al.* (2015): 5-HT1A receptors on mature dentate gyrus granule cells are critical for the antidepressant response. Nat Neurosci 18:1606–1616.
28. Reich M, Liefeld T, Gould J, Lerner J, Tamayo P, Mesirov JP (2006): GenePattern 2.0. Nat Genet 38:500–501.
29. Langfelder P, Horvath S (2008): WGCNA: An R package for weighted correlation network analysis. BMC Bioinformatics 9:559.

30. Habib N, Li Y, Heidenreich M, Swiech L, Avraham-Davidi I, Trombetta JJ, *et al.* (2016): Div-Seq: Single-nucleus RNA-Seq reveals dynamics of rare adult newborn neurons. Science 353:925–928.
31. Erwin SR, Sun W, Copeland M, Lindo S, Spruston N, Cembrowski MS (2020): A sparse, spatially biased subtype of mature granule cell dominates recruitment in hippocampal-associated behaviors. Cell Rep 31:107551.
32. Sillaber I, Panhuysen M, Henniger MS, Ohl F, Kühne C, Pütz B, *et al.* (2008): Profiling of behavioral changes and hippocampal gene expression in mice chronically treated with the SSRI paroxetine. Psychopharmacol (Berl) 200:557–572.
33. Zhang TY, Keown CL, Wen X, Li J, Vousden DA, Anacker C, *et al.* (2018): Environmental enrichment increases transcriptional and epigenetic differentiation between mouse dorsal and ventral dentate gyrus. Nat Commun 9:298.
34. Williams PA, Larimer P, Gao Y, Strowbridge BW (2007): Semilunar granule cells: Glutamatergic neurons in the rat dentate gyrus with axon collaterals in the inner molecular layer. J Neurosci 27:13756–13761.
35. Gupta A, Subramanian D, Proddutur A, Chang YJ, Guevarra J, *et al.* (2019): Semilunar granule cells maintain distinct dendritic morphology and inhibition through postnatal development and receive heightened inhibition in adolescence. bioRxiv. https://doi.org/10.1101/2019.12.17.880005.
36. Rao-Ruiz P, Couey JJ, Marcelo IM, Bouwkamp CG, Slump DE, Matos MR, *et al.* (2019): Engram-specific transcriptome profiling of contextual memory consolidation. Nat Commun 10:2232.
37. Amaral DG, Scharfman HE, Lavenex P (2007): The dentate gyrus: Fundamental neuroanatomical organization (dentate gyrus for dummies). Prog Brain Res 163:3–22.
38. Williams NR, Heifets BD, Bentzley BS, Blasey C, Sudheimer KD, Hawkins J, *et al.* (2019): Attenuation of antidepressant and antisuicidal effects of ketamine by opioid receptor antagonism. Mol Psychiatry 24:1779–1786.
39. Williams NR, Heifets BD, Blasey C, Sudheimer K, Pannu J, Pankow H, *et al.* (2018): Attenuation of antidepressant effects of ketamine by opioid receptor antagonism. Am J Psychiatry 175:1205–1215.
40. Joseph TT, Bu W, Lin W, Zoubak L, Yeliseev A, Liu R, *et al.* (2021): Ketamine metabolite (2R,6R)-hydroxynorketamine interacts with μ and κ opioid receptors. ACS Chem Neurosci 12:1487–1497.
41. Richards EM, Mathews DC, Luckenbaugh DA, Ionescu DF, Machado-Vieira R, Niciu MJ, *et al.* (2016): A randomized, placebo-controlled pilot trial of the delta opioid receptor agonist AZD2327 in anxious depression. Psychopharmacology (Berl) 233:1119–1130.
42. Porsolt RD, Le Pichon ML, Jalfre M (1977): Depression: A new animal model sensitive to antidepressant treatments. Nature 266:730–732.
43. Lucki I (1997): The forced swimming test as a model for core and component behavioral effects of antidepressant drugs. Behav Pharmacol 8:523–532.
44. Santarelli L, Saxe M, Gross C, Surget A, Battaglia F, Dulawa S, *et al.* (2003): Requirement of hippocampal neurogenesis for the behavioral effects of antidepressants. Science 301:805–809.
45. Drysdale AT, Grosenick L, Downar J, Dunlop K, Mansouri F, Meng Y, *et al.* (2017): Resting-state connectivity biomarkers define neurophysiological subtypes of depression [published correction appears in Nat Med 2017;23:264]. Nat Med 23:28–38.
46. Grosenick L, Shi TC, Gunning FM, Dubin MJ, Downar J, Liston C (2019): Functional and optogenetic approaches to discovering stable subtype-specific circuit mechanisms in depression. Biol Psychiatry Cogn Neurosci Neuroimaging 4:554–566.
47. Samuels BA, Mendez-David I, Faye C, David SA, Pierz KA, Gardier AM, *et al.* (2016): Serotonin 1A and serotonin 4 receptors: Essential mediators of the neurogenic and behavioral actions of antidepressants. Neuroscientist 22:26–45.
48. Qi X, Lin W, Li J, Li H, Wang W, Wang D, Sun M (2008): Fluoxetine increases the activity of the ERK-CREB signal system and alleviates the depressive-like behavior in rats exposed to chronic forced swim stress. Neurobiol Dis 31:278–285.
49. Erbs E, Faget L, Scherrer G, Kessler P, Hentsch D, Vonesch JL, *et al.* (2012): Distribution of delta opioid receptor-expressing neurons in the mouse hippocampus. Neuroscience 221:203–213.
50. Sagi Y, Medrihan L, George K, Barney M, McCabe KA, Greengard P (2020): Emergence of 5-HT5A signaling in parvalbumin neurons mediates delayed antidepressant action. Mol Psychiatry 25:1191–1201.
51. Larimer P, Strowbridge BW (2010): Representing information in cell assemblies: Persistent activity mediated by semilunar granule cells. Nat Neurosci 13:213–222.